Long-term *in vivo* imaging of experience-dependent synaptic plasticity in adult cortex

Joshua T. Trachtenberg*†, **Brian E. Chen***†, **Graham W. Knott**‡, **Guoping Feng**§, **Joshua R. Sanes**§, **Egbert Welker**‡ & **Karel Svoboda***

* *Howard Hughes Medical Institute, Cold Spring Harbor Laboratory, Cold Spring Harbor, New York 11724, USA*
‡ *Institut de Biologie Cellulaire et de Morphologie, Université de Lausanne, Rue du Bugnon 9, CH 1005, Lausanne, Switzerland*
§ *Department of Anatomy and Neurobiology, Washington University School of Medicine, St Louis, Missouri 63110, USA*
† *These authors contributed equally to this work*

....

Do new synapses form in the adult cortex to support experience-dependent plasticity? To address this question, we repeatedly imaged individual pyramidal neurons in the mouse barrel cortex over periods of weeks. We found that, although dendritic structure is stable, some spines appear and disappear. Spine lifetimes vary greatly: stable spines, about 50% of the population, persist for at least a month, whereas the remainder are present for a few days or less. Serial-section electron microscopy of imaged dendritic segments revealed retrospectively that spine sprouting and retraction are associated with synapse formation and elimination. Experience-dependent plasticity of cortical receptive fields was accompanied by increased synapse turnover. Our measurements suggest that sensory experience drives the formation and elimination of synapses and that these changes might underlie adaptive remodelling of neural circuits.

The cellular and synaptic mechanisms underlying experience-dependent plasticity in the adult neocortex are not understood[1–7]. In the most widely studied cellular model of plasticity, namely use-dependent potentiation and depression of synaptic transmission, synaptic connectivity is assumed to be fixed[8,9]. Another view holds that cortical plasticity results from a restructuring of neural circuits[10]; this is supported by studies documenting the growth of axonal and dendritic processes[6,11,12]. A separate model suggests changes in cortical connectivity at the level of individual synapses, without large-scale rearrangements of neuronal processes[13–15]. These models are probably not exclusive but might operate over distinct timescales[16].

Here we focus on dendritic spines as the substrate of plasticity. Spines are tiny dendritic protrusions that receive the vast majority of excitatory synapses[17,18]. In cultured preparations, spines grow in response to bursts of synaptic stimulation[19,20] and make synapses[21]. In the adult brain, spines can appear in response to hormonal changes[22] and prolonged sensory overstimulation[15]; during development, spines show experience-dependent structural plasticity[23]. Furthermore, theoretical studies have suggested that the formation and elimination of synapses through growth of spines constitute a potential memory mechanism with enormous information capacity[14].

Here we report that spines appear and disappear frequently in the adult cortex, whereas the growth or retraction of dendritic or axonal processes was not observed. Spine sprouting is associated with synapse formation, and spine retraction with synapse elimination. The rate of synaptic turnover is increased in response to novel sensory experience.

Imaging of dendritic spines in adult cortex

To determine whether synaptic connectivity in the adult cortex is fixed, or whether the formation and elimination of synapses occur, we developed a preparation for chronic high-resolution imaging of neuronal structure *in vivo*. We used mice expressing enhanced green fluorescent protein in a small subpopulation (~1%) of layer-5 pyramidal neurons[24]. Young adult mice (6–10 weeks of age) were prepared for imaging by implanting a small imaging window

centred over the barrel cortex (see Methods) (Fig. 1a). Two-photon laser-scanning microscopy[23,25,26] revealed fluorescent dendritic arbors, in a pattern of labelling that resembles a Golgi stain (Fig. 1b–e). Characteristically for layer-5 neurons, these arbors were in layers 1 and 2 (ref. 27). At higher magnifications, dendritic spines (Fig. 1f), axons and presynaptic terminals (see section 'New spines form synapses') could be imaged with high contrast. In a typical long-term experiment the same dendritic regions were imaged every day for 8 days and less frequently thereafter (Fig. 1f).

Dynamic spines in the adult cortex

Previous time-lapse imaging studies in the developing barrel cortex demonstrated that spines show rapid motility, and grow and retract over times of tens of minutes[23]. Relatively few changes were found over these periods in the adult cortex (see Methods). However, chronic time-lapse imaging revealed that spines were still dynamic, but over much longer timescales (see Fig. 1f). About 20% of spines disappeared between imaging sessions from one day to the next, balanced by the formation of new spines. About 60% of spines persisted for at least 8 days. We examined whether growth or retraction also occurred at the level of dendritic branching. Of 125 dendritic branches imaged at high magnification over timescales as long as 1 month (range 8–32 days), we failed to observe any branch additions or subtractions (Fig. 2). Similar conclusions hold for axonal branches that were sometimes apparent in our images (data not shown). Although we cannot rule out the possibility of very slow (less than μm per day) growth of dendritic and axonal branch tips, large-scale changes in the arrangement of neuronal processes do not occur and changes in dendritic structure are limited mainly to spines.

New spines form synapses

Does the growth and retraction of spines correspond to synapto-genesis and synapse elimination? To address this question we combined chronic *in vivo* imaging with ultrastructural analysis. Two dendritic regions that had been previously imaged for eight sequential days *in vivo* were identified in fixed tissue (Fig. 3A–D) and reconstructed using serial-section electron microscopy (SSEM;

Supplementary Information). The general appearance of these reconstructed dendrites (Fig. 3E), characterized by a relatively high proportion of shaft synapses and low spine densities, is consistent with previous work on layer 1 (ref. 28). One region of dendrite (length 29 μm) contained 22 synapses (18 asymmetric, 4 symmetric) (Fig. 3E) and two spines that had been observed to appear between the last two imaging sessions (days 7 and 8) (boxed

regions in Fig. 3D and E). The second region (not shown; length 21 μm) contained 17 synapses (14 asymmetric and 3 symmetric) and two spines that appeared between the last two imaging sessions. In total, 18 spines were reconstructed, 4 of which were new spines (less than 1 day old). Comparing SSEM reconstructions with the *in vivo* images showed that two new spines contained clear synapses (Fig. 3F and G). These spines contacted presynaptic boutons and
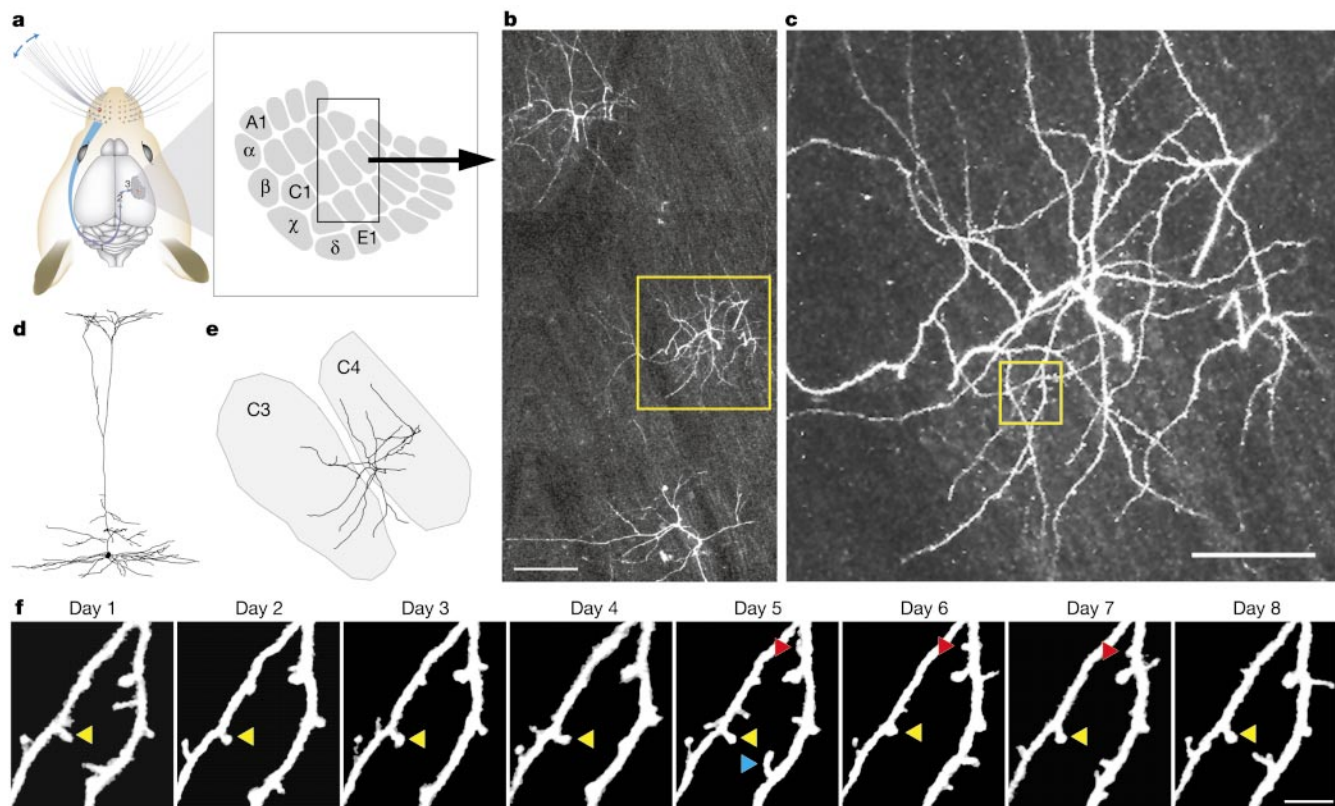

Figure 1 Chronic time-lapse imaging of dendritic spines in the barrel cortex *in vivo*.
a, Diagram of the barrel cortex and its topographic structure (boxed region, right). **b**, Low-magnification dorsal view of the apical dendrites of three layer-5 pyramidal neurons. Scale bar, 100 μm. **c**, Higher-magnification view of one apical tuft (yellow box in **b**). Scale bar, 50 μm. **d**, Neuron reconstructed from images of fixed sections obtained after collection of

the last vital image (same neuron as in **c**). **e**, Dorsal view of the reconstructed apical tuft, depicting the positions of each dendritic branch relative to the barrel map. **f**, High-resolution time-lapse images of a dendritic region (yellow box in **c**). Examples of transient, semi-stable and stable spines are labelled with blue, red and yellow arrowheads, respectively. Scale bar, 5 μm.
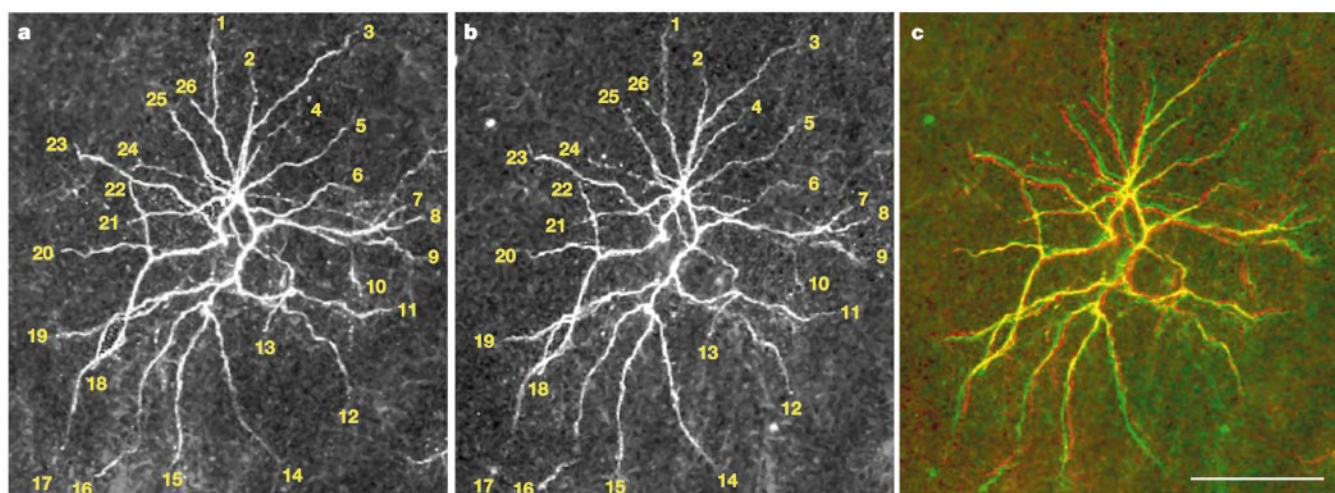

Figure 2 Dendritic branches are stable over weeks. **a**, Dorsal view of an apical tuft at imaging day 16; 26 branch tips are labelled for reference. **b**, Imaging day 32. **c**, Overlay (day 16, red; day 32, green). Scale bar, 100 μm.

were apposed to active zones containing clusters of synaptic vesicles (Fig. 3H and I). Thus, new spines in the adult brain make synapses.

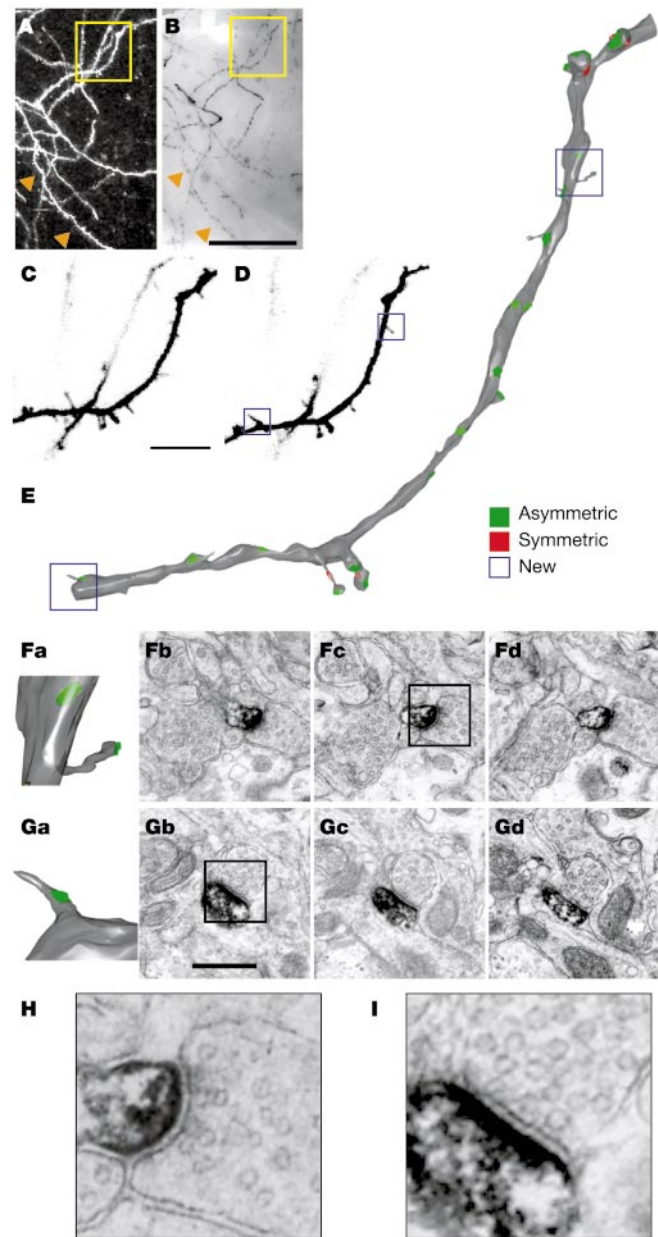Two views of the relationship between spine turnover and synapses are currently prominent. In the first, spines could grow to make new synapses[13,14]. In the second, spines could emerge just below an existing shaft synapse and drag this synapse along, in which case spine growth would not be associated with a gain of synapses[17].

Three lines of evidence support the first model. First, in two examples from two separate animals we observed spine growth towards axonal varicosities (Fig. 4). In these examples the varicosities were stable and were contacted, at the level of light microscopy, on two occasions by different spines emerging from the same dendrite. Second, if the formation of spines were to push synapses away from the dendritic shaft, local movements and changes in the curvature of axons would be observable. However, the trajectory of axons was remarkably constant (Fig. 4, and data not shown).

The third line of evidence comes from comparing the number of spines that retracted over 8 days of imaging with the number of shaft synapses observed in the SSEM reconstructions. If retracting spines did indeed pull their associated presynaptic bouton to establish shaft synapses, we would expect the number of shaft synapses to be greater than or equal to the number of retracted spines. We counted 17 excitatory shaft synapses in the two dendritic segments reconstructed by SSEM. In contrast, in these same dendritic regions we observed 28 spines that retracted over 8 days of imaging; the actual number of retracted spines is likely to be considerably larger because we cannot reliably resolve, and hence did not analyse, spines that project above and below the dendrite. Thus, the number of retracted spines is severalfold higher than the number of shaft synapses. Furthermore, of the retracted spines only seven were within $0.5\,\mu m$ of a shaft synapse. We conclude that retracting spines do not maintain synaptic contact. In addition, two spines that appeared between the last two imaging sessions seemed to be in various phases of synapse formation or elimination. One new spine clearly contacted an axon, although it lacked presynaptic specialization, and one spine did not show a clear indication of presynaptic contact in the SSEM sections (data not shown). Thus, *in vivo* imaging in combination with SSEM provides strong evidence for *de novo* synaptogenesis and synapse elimination in the adult neocortex.

Spines are distributed into kinetic classes

Our time-lapse images indicate that stable and dynamic spines are apparently intermixed along the dendrite (Figs 1f and 5a). Despite spine turnover, spine density was stable (Fig. 5b). To quantify the
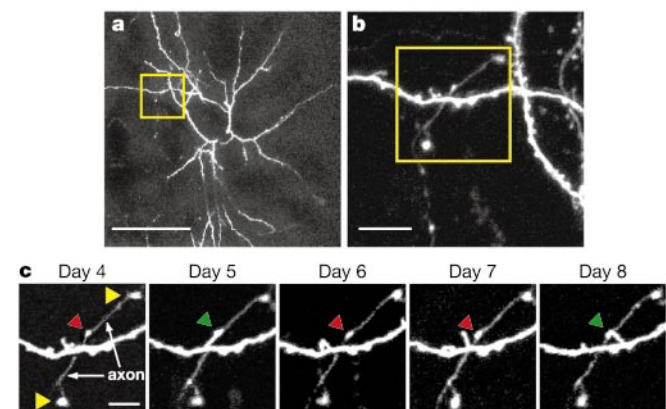

Figure 3 New spines establish synapses. **A**, *In vivo* image of a dendritic region on the eighth and final imaging day. **B**, The same dendritic region immunolabelled for green fluorescent protein in fixed tissue. Orange arrowheads identify the same dendrite in the two panels. The yellow box indicates the dendritic region that was serially reconstructed for electron microscopy. Scale bar, 50 μm. **C**, *In vivo* image (inverted), acquired on the seventh imaging day (yellow box in **A** and **B**). **D**, Same dendritic region as in **C** on the eighth imaging day, immediately before perfusion. Two new spines appeared after the seventh imaging day (boxes). Scale bar, 10 μm. **E**, Three-dimensional reconstruction of the dendritic region from serial-section electron micrographs. The red regions indicate symmetric (presumably inhibitory) synapses; the green regions asymmetric (presumably excitatory) synapses. The boxes delineate the same two new spines as in **D**. **Fa**, **Ga**, New spines identified by the upper-right and lower-left boxes in **E**, respectively. Green regions identify asymmetric synapses. **Fb–d**, **Gb–d**, Electron micrographs showing synapses established by these new spines. Scale bar, 0.5 μm. **H**, **I**, Enlargement of boxed regions of **Fc** and **Gb**, respectively, showing synaptic clefts and vesicle clusters. Scale bar, 0.125 μm.

Figure 4 *In vivo* imaging of putative synapse formation and elimination. **a**, Low-magnification image. Scale bar, 100 μm. **b**, Higher-magnification view (yellow box in **a**). Scale bar, 10 μm. **c**, Further magnified view (yellow box in **b**). An axon (day 4, white arrows) with varicosities (day 4, red and yellow arrowheads) is coursing across the dendrite. One varicosity (day 4, red arrowhead) seems to be contacted by a dendritic spine on two separate occasions (days 5 and 8). The transition of the arrowhead from red to green indicates the close apposition of the axon and two different dendritic spines, suggesting synapse formation. Scale bar, 5 μm.

kinetics of spine turnover we measured the lifetime of each spine as the number of sequential days over which a spine was present during an 8-day period (1224 spines, $n = 7$ cells, one cell per animal). The distribution of spine lifetimes revealed at least three kinetic components (Fig. 5c): transient spines appeared in only one image (lifetime ≤ 1 day); semi-stable spines persisted with a mean lifetime of 2–3 days (Fig. 5c; exponential fit to the central portion of the lifetime distribution); and stable spines survived the entire imaging period (lifetime ≥ 8 days). On any given day, transient spines make up ~17% of the spine population, semi-stable spines ~23% and stable spines 60%.

We examined whether stable spines are permanent or whether they, too, turn over with time. In three animals we imaged spines for eight sequential days and identified stable spines. We then imaged these same spines 20–24 days later (~30 days after the first imaging day). Of 157 spines that were present throughout the first eight imaging days, 132 were still present on day 30 (cf. Figure 5d, yellow arrowheads). A substantial fraction (~15%) of stable spines had therefore disappeared (cf. Figure 5d, orange arrowhead). An analysis of spine structure revealed that large spines (as judged by volume[29]) were more likely to be stable than transient spines (Supplementary Information). Large mushroom-shaped spines[30] were almost always stable for the entire duration of the experiment (for example, yellow arrowheads in Figs 1f and 5a, d).

Sensory experience modulates spine turnover

Are the addition and subtraction of spines influenced by sensory experience? To explore this question we altered sensory experience by trimming every other whisker on the mystacial pad, such that each trimmed whisker was surrounded by intact whiskers (Fig. 6a). This 'chessboard' deprivation produces an imbalance in the activation of neighbouring cortical columns, similar to the monocular deprivation used in the visual system[31], and induces a rapid and robust remodelling of whisker representation[32,33].

We tested whether the dynamics of spines is influenced by chessboard deprivation. In each mouse, whiskers were left intact for the first 4 days of imaging. Whiskers on the contralateral mystacial pad were then trimmed, and imaging continued for a further 4 days (Fig. 6a). A comparison of spine lifetime in the barrel cortex before and after deprivation revealed considerable experience-dependent effects (579 spines, $n = 4$ cells). Chessboard deprivation increased the pool of transient spines, present for only a single day or less, with a concomitant decrease in the pool of stable spines (Fig. 6b). This change was specific to deprived cortical areas, because no change in spine lifetimes was observed in cells outside the barrel cortex (645 spines, $n = 3$ cells; Fig. 6c). Sensory deprivation did not modulate spine density regardless of whether a cell was in the barrel cortex (Fig. 6d). The lifetime of spines is therefore experientially modulated and homeostatic mechanisms keep spine
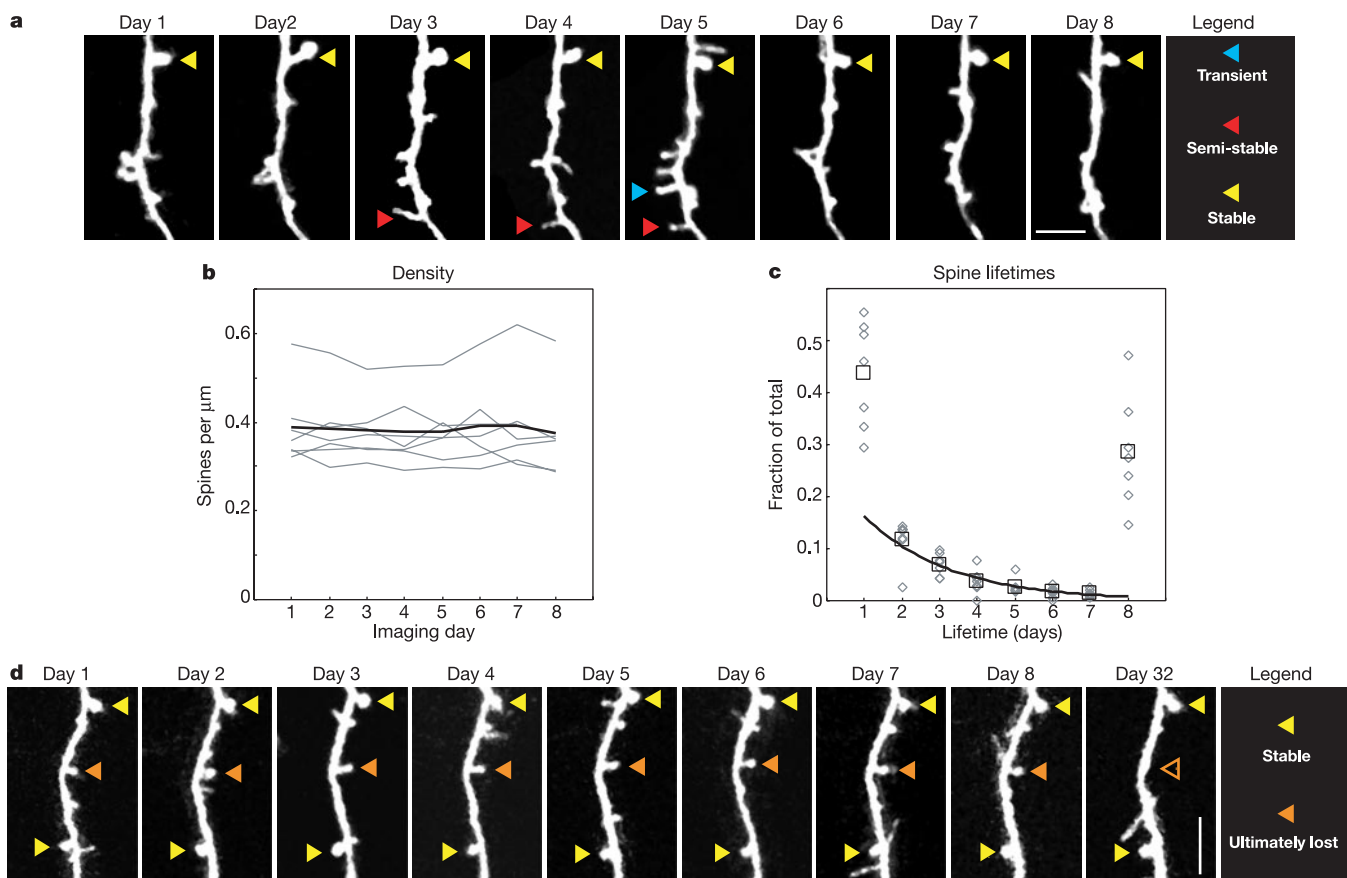

Figure 5 Spines appear and disappear with broadly distributed lifetimes, without changing spine density. **a**, Images of a dendritic segment acquired over eight sequential days. Examples of transient, semi-stable and stable spines (with lifetimes of ≤ 1 day, 2–7 days, and ≥ 8 days, respectively) are indicated with blue, red and yellow arrowheads, respectively. Scale bar, 5 μm. **b**, Spine density (spines per μm of dendritic length) is plotted for seven neurons (grey lines) for each imaging day; the average spine density is indicated by a black line. **c**, Distribution of spine lifetimes. Lifetimes are defined as the number of sequential days (from a total of eight) over which a spine existed. Individual neurons (grey diamonds) and the average (black squares) are shown. The fraction of spines with lifetimes of 2–7 days is fitted with a single time constant (thick black line). The fractions of spines with lifetimes of less than 1 day (transient spines) and greater than 8 days (stable spines) are significantly greater than predicted from the exponential fit, and therefore constitute distinct kinetic populations. **d**, Example of a stable spine that ultimately disappears. Two large mushroom spines, indicated by the yellow arrowheads, have lifetimes of ≥ 32 days, whereas a third spine, indicated by the orange arrowhead, persists for ≥ 8 days but disappears by day 32. Scale bar, 5 μm.

and synaptic densities constant.

To examine the time course of the onset of synaptic rearrangement in these cells, we measured the fraction of spines gained and lost from one day to the next (turnover ratio) throughout the control and experimental conditions (Fig. 6e). The turnover ratio was stable over the first four imaging days in which whiskers were intact. Chessboard deprivation for 24 h failed to induce a significant change in the fraction of spines gained or lost relative to the control period. However, 2–4 days after the onset of chessboard deprivation, significant increases occurred in spine turnover relative to both the control period and to the first 24 h after deprivation ($P < 0.05$ for each comparison; two-tailed t-test corrected for multiple comparisons). Consistent with input-specific plasticity was the observation that spine turnover was stable in cells lying outside the deprived barrel cortex (Fig. 6e).

Plasticity of receptive fields

To examine how synaptic circuits are modified in response to chessboard deprivation that induces changes in spine turnover (Fig. 6), we used membrane potential measurements[34–36] (Supplementary Information). Intracellular recordings were made from pyramidal neurons (four control mice and nine mice that had

experienced 3–4 days of chessboard deprivation). To determine the neuron's position in the barrel map and therefore its principal whisker, recorded neurons were subsequently identified in cytochrome-oxidase-stained sections and assigned to a barrel column[34]. The amplitudes of postsynaptic potentials evoked by deflections of individual whiskers were used to characterize receptive field organization (Fig. 7a). In control animals, the structure of receptive fields resembled those of receptive fields previously measured in rats (Fig. 7b)[34–36]. Neurons responded most strongly to the principal whisker and more weakly to stimulation of first-order and second-order surround whiskers. In chessboard-deprived animals, neurons in barrels with their principal whisker trimmed had a significantly enhanced surround receptive field, corresponding to spared whiskers (Wilcoxon signed-rank test, $P < 0.05$). These measurements show that experience-dependent reorganization of synaptic circuits underlies receptive field plasticity. This is consistent with a role for synapse formation and elimination as the cellular mechanism underlying experience-dependent plasticity.

Discussion

A central question in neuroscience is how and to what extent neurons and their synapses change to support experience-dependent functional changes in the adult neocortex. To address this issue we used two-photon laser-scanning microscopy for chronic imaging of layer-5 pyramidal cell axons, dendrites and their spines in the barrel cortex *in vivo* (Fig. 1). We find that spines appear and disappear over periods of days to weeks, even though their average density remains constant (Fig. 5). In contrast, the large-scale branching pattern of dendrites and axons was stable (Fig. 2). To determine whether the sprouting and retraction of spines contribute to the rearrangement of cortical synaptic circuits, we directly correlated time-lapse images of dendritic spines *in vivo* with SSEM reconstructions of the same structures (Fig. 3). These measurements demonstrate that spine sprouting is associated with synapse formation, and spine retraction with synapse elimination. Synaptogenesis is therefore not limited to development but also occurs at
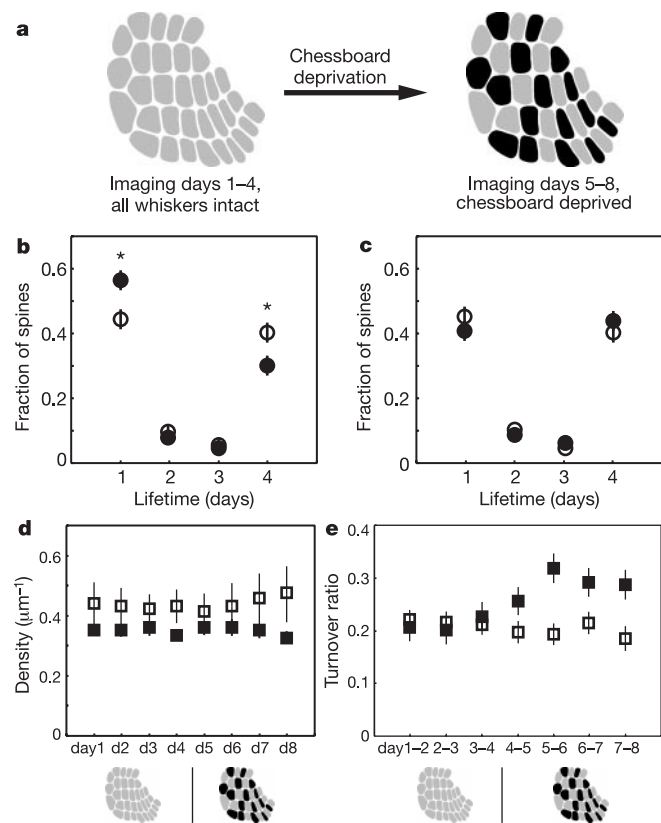

Figure 6 Altering sensory experience increases spine turnover rates. **a**, Experimental protocol (see text). Black barrels are deprived. **b**, Distribution of spine lifetimes (over four imaging days) for control (open circles) and chessboard-deprived (solid circles) conditions for cells within the barrel cortex. Asterisks indicate significantly different populations. Deprivation reduces the fraction of spines with longer lifetimes and increases the number of transient spines. **c**, Spine lifetimes for neurons outside the barrel cortex. Deprivation does not change spine lifetimes. Symbols as in **b**. **d**, Spine density for cells lying within (solid squares) or outside (open squares) the barrel cortex. Spine density does not change in response to deprivation. **e**, Turnover ratio (the fraction of spines that turn over between successive imaging sessions) as a function of time. Chessboard deprivation occurred immediately after imaging day 4. Turnover ratio increased after deprivation within (solid squares) but not outside (open squares) the barrel cortex. Error bars in **b**–**e** show s.e.m.
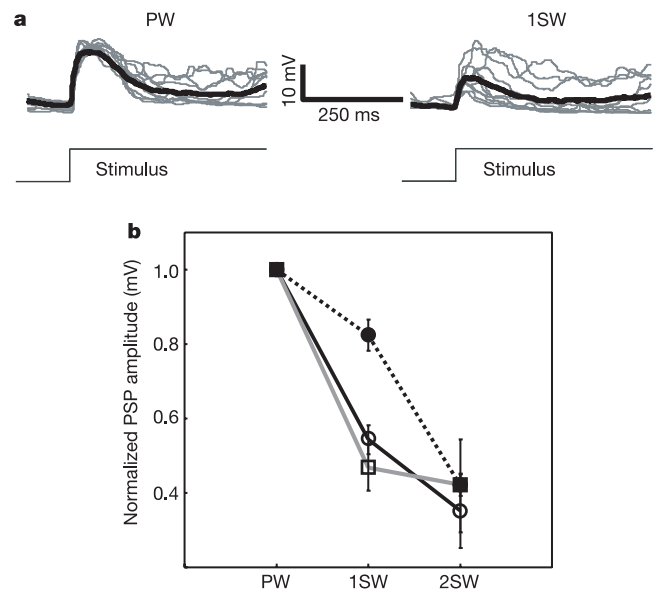

Figure 7 Experience-dependent receptive field plasticity. **a**, Examples of postsynaptic potentials (grey lines) and averages (thick black lines) evoked by stimulation of principal whisker (PW) and first-order surround whisker (1SW). **b**, Normalized evoked postsynaptic potential (PSP) amplitudes (means ± s.e.m.) for PW and surround whiskers (1SW, 2SW, first-order and second-order surround whiskers, respectively) for cells in control (black line), spared (grey line) and deprived (dotted line) barrels.

high rates in the adult brain. Reports of stable synaptic densities in the adult neocortex should not be viewed as the absence of synaptogenesis but rather as balanced rates of synapse formation and elimination[37,38].

We find that synaptic lifetimes are distributed broadly (Fig. 5). About 80% of synapses were detectable for a day or longer; about 60% belonged to the stable pool imaged for at least 8 days. Even this stable pool was found to turn over, with only ~50% of spines surviving for 30 days or longer. Assuming stochastic behaviour, we estimate that the mean lifetime of the stable pool would be on the order of 120 days. However, even longer imaging experiments might reveal that a subpopulation of synapses persists for the entire lifetime of the animal. Furthermore, our data indicate that synaptic stability is correlated with spine structure: larger spines tended to be more stable, and large mushroom spines were particularly so (Supplementary Information). Future experiments combining in vivo imaging with SSEM might reveal the ultrastructural determinants of synapse stability.

Our data are consistent with a model in which adaptive change in the adult neocortex occurs through changes in connectivity patterns through the sprouting and retraction of dendritic spines, without large-scale rearrangements of neuronal processes. Similar changes have been observed previously in developing brain slices[19–21] and in the developing barrel cortex[23], as well as in response to long-term overstimulation of whiskers in the adult cortex[15]. New synapses could strengthen previously existing connections or connect previously unconnected neurons.

To determine whether synapse addition and subtraction might be involved in experience-dependent plasticity, we correlated receptive field changes with chronic imaging of dendritic spines. We find that after 2–4 days of sensory deprivation the turnover of spines increases markedly (Fig. 6), coincident with rearrangements of receptive field structure as probed by maps of excitatory synaptic potentials (Fig. 7). Taken together, our data suggest that changes in synaptic connectivity might underlie experience-dependent rewiring of the adult brain.

What is the role of transient synapses in experience-dependent rearrangements of cortical circuits? Our data are consistent with the following model. Spines sample (perhaps randomly) presynaptic partners from the set of available presynaptic partners (potential synapses)[14]. Appropriate synapses might then be stabilized in an activity-dependent manner, and other synapses are eliminated. In this model the transient increase in synapse turnover after the onset of deprivation is the consequence of destabilization of previously stable synapses.

Our results have relevance to understanding the mechanisms underlying the closure of critical periods. Critical periods, first characterized in the primary visual cortex[39], are temporal windows in postnatal development when experience profoundly influences the final organization of neural connections. Although we report a high rate of synaptogenesis and synapse elimination in the adult cortex that is regulated by experience, all of these synaptic changes are local, without growth or elimination of axons or dendritic branches, using a fixed complement of potential synapses. This is in profound contrast to critical period plasticity, which has been documented to be associated with changes at the level of axonal[40] and dendritic branching (M. Maravall & K.S., unpublished observations). The cessation of such process growth might bring critical periods to a close. This would ensure that plasticity induced in the adult cortex would be reversible, because the original presynaptic partners remain in place, as do the major dendritic branches. In contrast, plasticity induced and maintained throughout the duration of a critical period would be irreversible in the adult because axonal and dendritic branch growth and retraction would fundamentally restructure the circuit. □

Methods

Surgery

Male c57/Bl6 transgenic mice (postnatal day (PND) 34–74) expressing enhanced green fluorescent protein in a subset of cortical-layer-5 pyramidal neurons (transgenic line M; ref. 24) were used for this study. Mice were deeply anaesthetized with an intraperitoneal injection of ketamine (0.13 mg per g body weight) and xylazine (0.01 mg g^{-1}). Dexamethasone (0.02 ml at 4 mg ml^{-1}) was administered subcutaneously. A 5×5 mm^2 region of the skull was removed, exposing the dura. An optical chamber was then constructed by covering the intact dura with agarose (Sigma, catalogue no. A9793) and a custom-made cover glass (no. 1), sealed with dental acrylic. A small titanium bar with tapped screw holes was embedded into the acrylic to stabilize the animal for subsequent imaging sessions. Animals were returned to their cages after surgery and allowed 7–10 days to recover before daily imaging began.

Imaging

In vivo images of neurons expressing green fluorescent protein were acquired as described[23] by using a 40×0.8 numerical aperture objective lens (Zeiss) and custom image-acquisition software (MatLab). For chronic experiments, animals were lightly anaesthetized with ketamine/xylazine at half the surgical dose (see above). At this level, anaesthesia typically wore off within 30 min, at which time animals were again returned to their cage. In acute experiments, performed in anaesthetized animals over durations of hours, we saw few changes (Supplementary Information). The apical dendrites of single layer-5 pyramids (three to eight fields, $45 \times 45\,\mu\text{m}^2$) were imaged daily over periods of 8–10 days and less frequently thereafter. Care was taken with each imaging session to achieve similar fluorescence levels. Imaged dendrites were within $100\,\mu\text{m}$ of the pia and were therefore in layer 1. Standard histological techniques were used to determine whether individual neurons were in the barrel cortex[34].

Image analysis was done blind with regard to experimental condition. For every image stack a single montage image was created, composed of the best focal plane for each spine. The montage images were then aligned by using fiducial marks that were stable across all imaging days. The presence or absence of each spine was recorded each day and spine positions along the dendrites were measured. Turnover ratios were calculated as $(N_{\text{gained}} + N_{\text{lost}})/(2N_{\text{total}})$, where N_{gained} is the number of new spines, N_{lost} is the number of lost spines, and N_{total} is the total number of spines. Turnover ratios were indistinguishable in animals in which experiments were initiated at PND 34 or 74, indicating that, in terms of spine dynamics, our measurements report the adult state.

To determine whether spine densities (Figs 5b and 6d) changed over time, linear regression lines were fitted to the density plots for each cell. The significance of the difference between means of daily turnover rates (Fig. 6e) was determined with a Student's two-tailed t-test. To correct for multiple comparisons the reported P value was calculated as $1 - (1 - P)^n$, where n is the number of comparisons. To determine whether spine lifetimes were significantly different before and after chessboard deprivation, we calculated the predicted standard deviation in spine lifetimes from the binomial distribution as $\sqrt{[nP(1 - P)]}$. Significance was set at $P = 0.05$.

The axial resolution of optical microscopy is relatively poor[41]. We have therefore not analysed spines that projected mainly along the optical axis. Spines vary greatly in volume[42] and therefore fluorescence intensity (~50-fold; Supplementary Information), the smallest spines being close to the detection limit. However, we are confident that we reliably detected even the smallest protrusions in our in vivo imaging. First, the spine density in our in vivo images (Fig. 6d) is not different from measurements in fixed tissue from the same animals ($0.48 \pm 0.16\,\mu\text{m}^{-1}$). Second, even the smallest structures reconstructed in SSEM were also detected in our in vivo images (Fig. 3F and G). The converse was also true: spines that disappeared in time-lapse imaging were confirmed as absent in three-dimensional SSEM reconstructions ($n = 6$ spines). It is therefore unlikely that an apparent loss of spines corresponds to changes in the imaging conditions or to local torsions of the dendritic shaft.

To check for possible effects of the cranial window on the health of cortical circuits we conducted several control experiments. We performed measurements of membrane potential directly below the window, in animals that had had windows implanted 2 weeks before recording, and compared these measurements with those from age-matched controls (see below). As a measure of the health of cortical circuitry we recorded spontaneous synaptic activity and characterized the amplitudes of spontaneous fluctuations in membrane potential[23,34]. We found that the amplitudes of membrane fluctuations (characterized as the s.d.) were identical in implanted animals (4.6 ± 2.6 mV; $n = 9$) and controls (5.0 ± 1.7 mV; $n = 9$), suggesting that our implants did not perturb the underlying cortical circuits. Consistently, densities of spines measured in fixed brains were not different from densities immediately below the imaging window and spine densities did not vary with experimental duration (Figs 5b and 6d). Finally, SSEM analysis of layer 1 did not show evidence for the proliferation of glial cells or other indications of tissue damage (Supplementary Information).

Electron microscopy and electrophysiology

To study the ultrastructure of the imaged dendrites, a pre-embedding immunolabelling protocol was used[43]. Identified cells were drawn with Neurolucida software (Microbrightfield) and the relevant dendrites were serially sectioned and photographed under the electron microscope for three-dimensional reconstructions (Supplementary Information). Measurements of subthreshold receptive fields were performed on wild-type c57/bl6 5-week-old male mice ($n = 13$) essentially as described[34] (Supplementary Information).

1. Squire, L. R. & Alvarez, P. Retrograde amnesia and memory consolidation: a neurobiological

perspective. *Curr. Opin. Neurobiol.* **5,** 169–177 (1995).

2. Jenkins, W. M., Merzenich, M. M., Ochs, M. T., Allard, T. & Guic-Robles, E. Functional reorganization of primary somatosensory cortex in adult owl monkeys after behaviorally controlled tactile stimulation. *J. Neurophysiol.* **63,** 82–104 (1990).

3. Bakin, J. S. & Weinberger, N. M. Classical conditioning induces CS-specific receptive field plasticity in the auditory cortex of the guinea pig. *Brain. Res.* **536,** 271–286 (1990).

4. Gilbert, C. D. & Wiesel, T. N. Receptive field dynamics in adult primary visual cortex. *Nature* **356,** 150–152 (1992).

5. Diamond, M. E., Huang, W. & Ebner, F. F. Laminar comparison of somatosensory cortical plasticity. *Science* **265,** 1885–1888 (1994).

6. Florence, S. L., Taub, H. B. & Kaas, J. H. Large-scale sprouting of cortical connections after peripheral injury in adult macaque monkeys. *Science* **282,** 1117–1121 (1998).

7. Wang, X., Merzenich, M. M., Sameshima, K. & Jenkins, W. M. Remodelling of hand representation in adult cortex determined by timing of tactile stimulation. *Nature* **378,** 71–75 (1995).

8. Tanzi, E. I fatti i le induzione nell'odierna istologia del sistema nervoso. *Riv. Sper. Freniatr.* **19,** 419–472 (1893).

9. Martin, S. J., Grimwood, P. D. & Morris, R. G. Synaptic plasticity and memory: an evaluation of the hypothesis. *Annu. Rev. Neurosci.* **23,** 649–711 (2000).

10. Ramon y Cajal, S. Neue Darstellung vom histologischen Bau des Centralnervensystems. *Arch. Anat. Physiol. Anat. Abt. Suppl.*, 319–428 (1893).

11. Darian-Smith, C. & Gilbert, C. D. Axonal sprouting accompanies functional reorganization in adult cat striate cortex. *Nature* **368,** 737–740 (1994).

12. Volkmar, F. R. & Greenough, W. T. Differential rearing effects on rat visual cortical plasticity. *Science* **176,** 1445–1447 (1972).

13. Ziv, N. E. & Smith, S. J. Evidence for a role of dendritic filopodia in synaptogenesis and spine formation. *Neuron* **17,** 91–102 (1996).

14. Stepanyants, A., Hof, P. R. & Chklovskii, D. B. Geometry and structural plasticity of synaptic connectivity. *Neuron* **34,** 275–288 (2002).

15. Knott, G. W., Quairiaux, C., Genoud, C. & Welker, E. Formation of dendritic spines with GABAergic synapses induced by whisker stimulation in adult mice. *Neuron* **34,** 265–273 (2002).

16. Bailey, C. H. & Kandel, E. R. Structural changes accompanying memory formation. *Annu. Rev. Physiol.* **55,** 397–426 (1993).

17. Harris, K. M. Structure, development, and plasticity of dendritic spines. *Curr. Opin. Neurobiol.* **9,** 343–348 (1999).

18. Nimchinsky, E. A., Sabatini, B. L. & Svoboda, K. Structure and function of dendritic spines. *Annu. Rev. Physiol.* **64,** 313–353 (2002).

19. Maletic-Savatic, M., Malinow, R. & Svoboda, K. Rapid dendritic morphogenesis in CA1 hippocampal dendrites induced by synaptic activity. *Science* **283,** 1923–1927 (1999).

20. Engert, F. & Bonhoeffer, T. Dendritic spine changes associated with hippocampal long-term synaptic plasticity. *Nature* **399,** 66–70 (1999).

21. Toni, N., Buchs, P. A., Nikonenko, I., Bron, C. R. & Muller, D. LTP promotes formation of multiple spine synapses between a single axon terminal and a dendrite. *Nature* **402,** 421–425 (1999).

22. Yankova, M., Hart, S. A. & Woolley, C. S. Estrogen increases synaptic connectivity between single presynaptic inputs and multiple postsynaptic CA1 pyramidal cells: A serial electron-microscopic study. *Proc. Natl Acad. Sci. USA* **98,** 3525–3530 (2001).

23. Lendvai, B., Stern, E., Chen, B. & Svoboda, K. Experience-dependent plasticity of dendritic spines in the developing rat barrel cortex *in vivo*. *Nature* **404,** 876–881 (2000).

24. Feng, G. *et al.* Imaging neuronal subsets in transgenic mice expressing multiple spectral variants of GFP. *Neuron* **28,** 41–51 (2000).

25. Denk, W., Strickler, J. H. & Webb, W. W. Two-photon laser scanning microscopy. *Science* **248,** 73–76 (1990).

26. Denk, W. & Svoboda, K. Photon upmanship: why multiphoton imaging is more than a gimmick. *Neuron* **18,** 351–357 (1997).

27. Kim, H. G. & Connors, B. W. Apical dendrites of the neocortex: correlation between sodium- and calcium-dependent spiking and pyramidal cell morphology. *J. Neurosci.* **13,** 5301–5311 (1993).

28. Vaughn, J. E. & Peters, A. A three dimensional study of layer I of the rat parietal cortex. *J. Comp. Neurol.* **149,** 355–370 (1973).

29. Svoboda, K., Tank, D. W. & Denk, W. Direct measurement of coupling between dendritic spines and shafts. *Science* **272,** 716–719 (1996).

30. Harris, K. M., Jensen, F. E. & Tsao, B. Three-dimensional structure of dendritic spines and synapses in rat hippocampus (CA1) at postnatal day 15 and adult ages: implications for the maturation of synaptic physiology and long-term potentiation. *J. Neurosci.* **12,** 2685–2705 (1992).

31. Wiesel, T. N. The postnatal development of the visual cortex and the influence of environment. *Nature* **299,** 583–591 (1982).

32. Glazewski, S., McKenna, M., Jacquin, M. & Fox, K. Experience-dependent depression of vibrissae responses in adolescent rat barrel cortex. *Eur. J. Neurosci.* **10,** 2107–2116 (1998).

33. Fox, K. Anatomical pathways and molecular mechanisms for plasticity in the barrel cortex. *Neuroscience* **111,** 799–814 (2002).

34. Stern, E., Maravall, M. & Svoboda, K. Rapid development and plasticity of layer 2/3 maps in rat barrel cortex in vivo. *Neuron* **31,** 305–315 (2001).

35. Zhu, J. J. & Connors, B. W. Intrinsic firing patterns and whisker-evoked synaptic responses of neurons in the rat barrel cortex. *J. Neurophysiol.* **81,** 1171–1183 (1999).

36. Moore, C. I. & Nelson, S. B. Spatio-temporal subthreshold receptive fields in the vibrissa representation of rat primary somatosensory cortex. *J. Neurophysiol.* **80,** 2882–2892 (1998).

37. Huttenlocher, P. R., de Courten, C., Garey, L. J. & Van der Loos, H. Synaptogenesis in human visual cortex—evidence for synapse elimination during normal development. *Neurosci. Lett.* **33,** 247–252 (1982).

38. Rakic, P., Bourgeois, J. P., Eckenhoff, M. F., Zecevic, N. & Goldman-Rakic, P. S. Concurrent overproduction of synapses in diverse regions of the primate cerebral cortex. *Science* **232,** 232–235 (1986).

39. Hubel, D. H. & Wiesel, T. N. Single-cell responses in striate cortex of kittens deprived of vision in one eye. *J. Neurophysiol.* **26,** 1003–1017 (1963).

40. Antonini, A. & Stryker, M. P. Rapid remodeling of axonal arbors in the visual cortex. *Science* **260,** 1819–1821 (1993).

41. Sandison, D. R., Piston, D. W. & Webb, W. W. *Three-Dimensional Confocal Microscopy: Volume Investigation of Biological Specimens* (eds Stevens, J. K., Mills, L. R. & Trogadis, J. E.) 29–47 (Academic, New York, 1994).

42. Harris, K. M. & Stevens, J. K. Dendritic spines of CA1 pyramidal cells in the rat hippocampus: serial electron microscopy with reference to their biophysical characterisitcs. *J. Neurosci.* **9,** 2982–2997 (1989).

43. Dunaevsky, A., Blazeski, R., Yuste, R. & Mason, C. Spine motility with synaptic contact. *Nature Neurosci.* **4,** 685–686 (2001).